Spectral Analysis of the Magnetic Residual Anomalies over the Upper Sokoto Basin, Nigeria

SHEU, A.T.; *UDENSI.E.E.; *ADENIYI, J.O.; AND JONAH, S.A.

Federal government college, Minna, Niger State.

**Physics Department, Federal University of Technology, Minna, Niger State.*

Abstract

Spectral analysis of the magnetic residual anomalies over the upper Sokoto Basin northwestern Nigeria was carried out to estimate the average depth to the basement magnetic rock in the area. The study area extends from latitude 12° 30'N to 12° 30'N and longitude 4° 00'E to 6°00'E and is covered by eight half degree aeromagnetic maps. The maps were digitized on a 2 km x 2 km grid and later combined to produce a composite magnetic map of the area. The least square polynomial fit method was applied in the region-residual separation. The observed magnetic residual anomalies over the study area was divided up into 60 sections, each of 14 x 14 overlapping grid blocks, for the purpose of analysis and interpretation. The spectral plots reveal two layers of magnetic sources. The first layer varies from 0.10km to 0.61km while the second layer depth is rather small to allow for the accumulation of hydrocarbons.

Introduction

The study area covers the Upper Basin in the northwestern part of Nigeria, Fig 1. The Sokoto Basin of northwestern Nigeria consists predominantly of a gentle undulating plain, underlain by metamorphic rocks. The study area is covered by eight (8) aeromagnetic maps. The maps were numbered 8,9,10,11,27,28,29 and 30. and the names of the places each map covers were also written on them for easy reference.

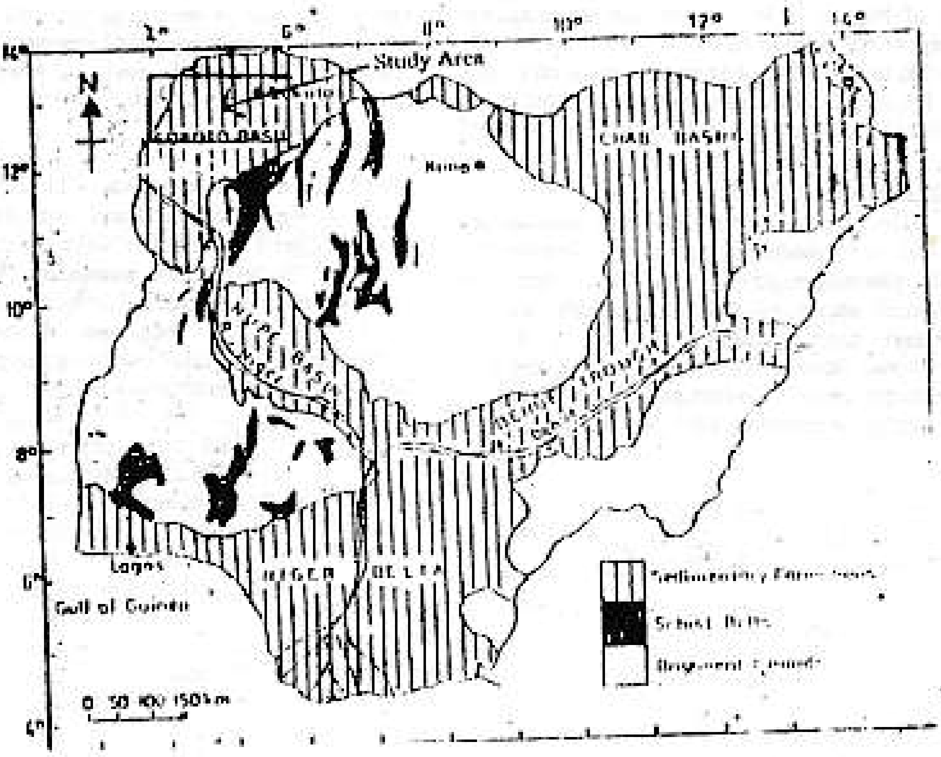

Fig 1: Simplified Geological Map of Nigeria Showing the Study Area

These maps were obtained from geological Survey of Nigeria (GSN) which carried out on aeromagnetic survey of substantial part of Nigeria between 1974 and 1980. The data were collected at a nominal flight altitude 0f 151m along N-S Flight lines spaced approximately 2km apart. The maps are on a scale of 1: 100,000 and half degree with a cotour interval of 10 gammas. The regional correction applied to the aeromagnetic data was based on the international Geomagnetic Reference Field (IGRF) epoch data of 1st January 1974.

Geological work in the Sokoto Basin dates back to late 1800's. Most of the published materials from this work relate to general geologic descriptions fossil localities, electromagnetic and seismic refraction surveys in different parts of the Basin. The surveys were aimed at studying the aquifers of basin with a view to selecting favourable sites for ground water boreholes. The results of these surveys have been published in form of Bulletins or as a special publication (Raeburn and Tattan, 1930). Unfortunately only one or two of the numerous boreholes scattered over the basin is/are known to have the basement and, as such, depth to basement estimates have been by extrapolations.

Between 1974 and 1980 the Geological survey of Nigeria (GSN) carried out aeromagnetic mapping of the Sokoto Basin, and the result of the survey has been published as contour maps on a scale of 1 : 100,000. Sokoto basin has not attracted much geophysical attention apparently because of the belief that no proven hydrocarbon accumulation or resource potentials have been indicated in the area. Umego (1990) carried out a gravity survey over part of the basin, and this was complemented by the analysis of the aeromagnetic data over the basin area. He compared the result obtained from gravity and magnetic analysis and noted a significant differences in the depth to basement estimates from both methods, the magnetic depth to basement estimates being generally larger. For example the maximum depth to basement estimates through gravity method was 1.0 km at one of the depressions, while the magnetic methods yielded estimate of 1.4km at the same location. At another location comparisons showed estimate of 0.8km and 1.6km for the gravity and magnetic methods respectively. Because of these significant differences, he suggested that boreholes and seismic information would considerably assist in constraining the model. Between 1964 and 1967 a United Nations project involving the use of aeromagnetic, aero electromagnetic, electrical, and magnetic methods was carried out in the study area. The survey was in search of minerals. The results showed that no important primary deposits of precious or base metals could be found within the area covered (Umego, 1990).

Geological Background

The Upper Sokoto Basin is a sedimentary basin with gentle undulating plain varying from 200 to 400 above sea level. The basin form the southeastern sector of the large, nearly circular sedimentary basin, generally referred to as the "Iullemmeden Basin" of West Africa, fig 2. the term "Iullemmeden basin" was first proposed by Raider in 1931 to define sedimentary basin which extends from Mali and the western boundary of the Republic of Niger through northern Benin Republic and north western Nigeria into Eastern Niger and covers an area of about 700,000 square kilometers (Kogbe,1979). The rock units are predominantly clay altering with gritty sand units, they are ill-sorted, poorly consolidated with gravel overlying the pre-Cambrian basement unconformable.

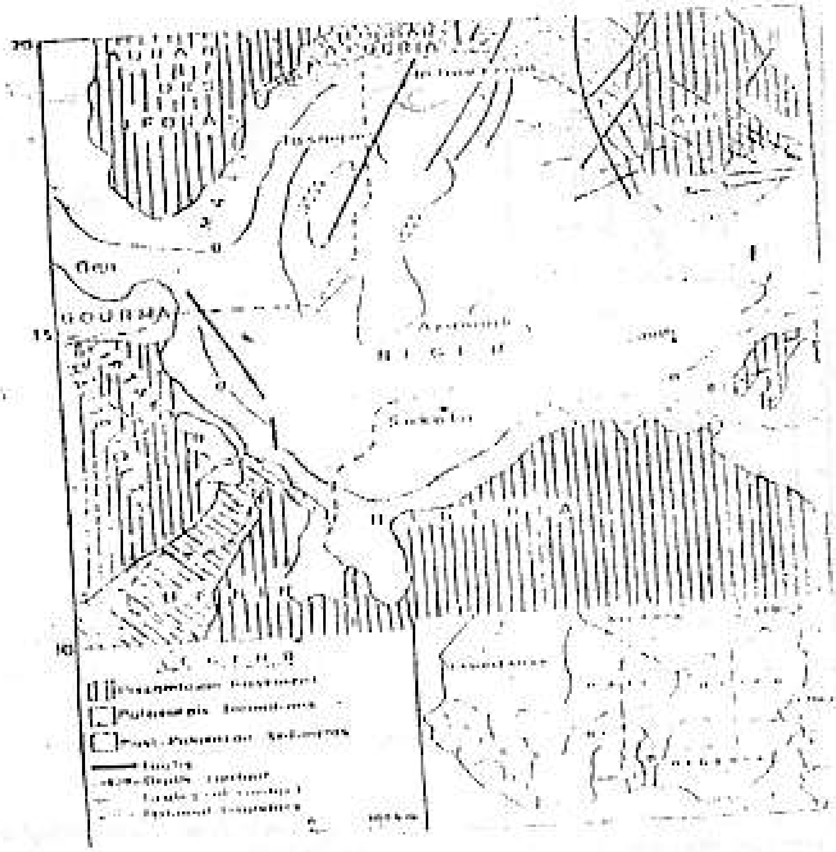

Fig. 2: Structural Map of the Iullemmedan Basin (After Kogbe 1979)

Data Manipulation

Digitization

The grid layout may be in rectangular form or square shape depending to a large extent on the wishes of the interpreter and the nature of the area concerned. Digitization on grid layout by visual interpolation was used in collecting magnetic field values on ½° x ½° aeromagnetic maps which are of dense magnetic contour by drawing twenty-eight (28) straight lines vertically and horizontally at equal spacing on tracing paper to form a layout of 2 x 2km² grid system. The boundaries of the layout coincided with the boundaries of the aereomagnetic map and the was then used for digitization. The layout over land on the aeromagnetic map and magnetic values are read at the intersections or cross points on the grid system. At the grid point where contour line was made so as to estimate the magnetic value at the grid point. Since the grid points were evenly spaced, it is easy to determine the longitude and latitude of each grid point.

Digitization on grid layout, by visual interpolation was used because tapes containing the original digital data recorded during the aeromagnetic survey could not be obtained from the Geological Survey of Nigeria. In all eight maps were digitized. These are 8,9,10,11,27,28,29 and 30 as shown in fig 3.

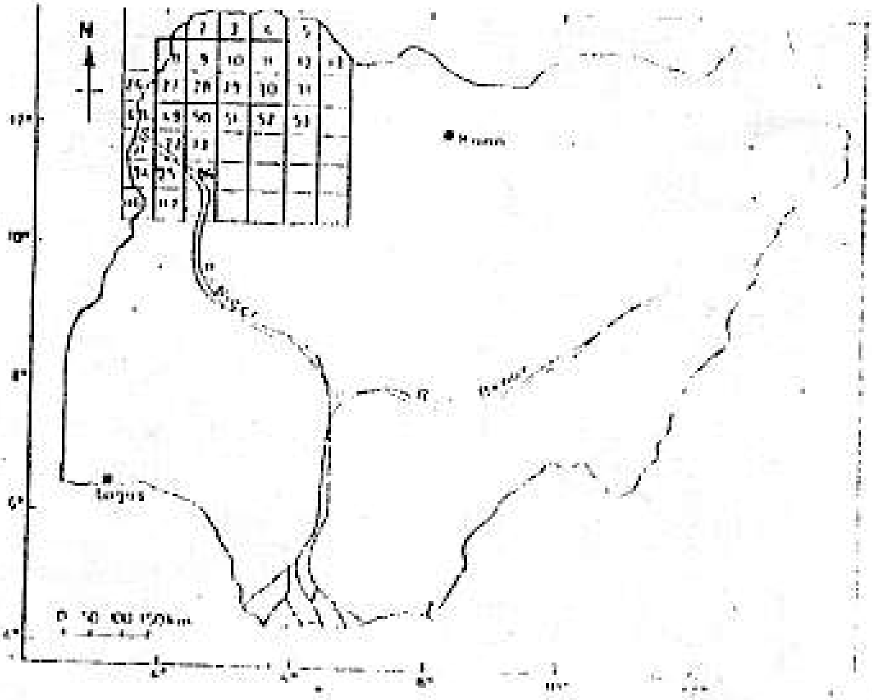

Fig. 3: Layout of half degree mps used in the study

After digitizing the aeromagnetic map the interpolated data from each map were then stored in 28 by 28 coding sheets. Each coding sheet contains name of the town overflown. The number and the boundary longitudes and latitudes. A computer program was written to read in and reproduce the date as they are contained in each coding sheet. To ensure that no mistake was made during input process into the computer the output data were compared with the input data. The output date contains magnetic values stating longitude and latitude of each map. This date file thereafter was used as the input file for another program that would pick all the data points row by row, calculate their latitudes and longitudes and produce the result in three columns (X,Y,Z). X,Y and Z represent longitude, latitude and magnetic values for the coordinates respectively. The three dimensional co-ordinate form x,y,z is the form that is acceptable to a contouring package "SUFER". Surfer is a menu driven interactive computer programme which places each magnetic data points according to their latitude and longitude bearing and thereafter produces a contour map for each of the eight aeromagnetic map.

The Production of Dataset and Unified Aeromagnetic Map for the Study Area

The interpolated data recorded on the coding sheets for each map were merged together column to column and row to row as contained in fig 4. to produce a unified dataset which in turn will be used to generate combined aeromagnetic map (unified map). The problem of boundary (edge) effect was solved by adding all magnetic values with the same co-ordinate and then averaging them so their there would not be rows and columns of magnetic points with the same co-ordinates. Fig 4. represent a rectangular outline of the upper Sokoto Basin with each number in the figure representing a topographic map sheet measuring 30' by 30' on the sexagesimal scale and contains 28 by 28 (784) digitized magnetic values.

8	9	10	11
27	28	29	30

Fig 4: Study Area Consising of 8nAeromgnetic Maps

At the boundary of two maps, for example maps 8 and 9, the magnetic field values in the last column of map 8 have the same coordinates (latitude and longitude) as the field values at the first column of map 9. This also occurs between maps 9 and 10 and between maps 10 and 11. Magnetic values at these points of same coordinates were added and averaged to get mean values at the edge in column forming 109 columns. Also at the boundary between map 8 and map 27 (for example) the magnetic field values at the last row of map 27. this also occurs between maps 9 and 28, 10 and 29 and maps 11 and 30. these points of the same co-ordinates were also added and averaged to get mean values at the boundary in row forming 55 rows. At the end of this manual merging method a total of 55 by 109 magnetic values (5995). These values were keyed into the computer as the unified dataset for this research work.

The unified dataset are magnetic values without coordinates. Thus before a unified map was produced from these dataset a computer programme was applied which read the data points row by row and calculated their latitudes and longitude using based values already supplied in aeromagnetic way. The output is in the form of columns of x,y,z where x,y and z represent longitude, latitude and the magnitude value of the given data point respectively. The output file in columns x,y,z were then used as an input file for the computer contouring package (SURFER) which produce a unified aeromagnetic map of the area as shown in Fig 5.

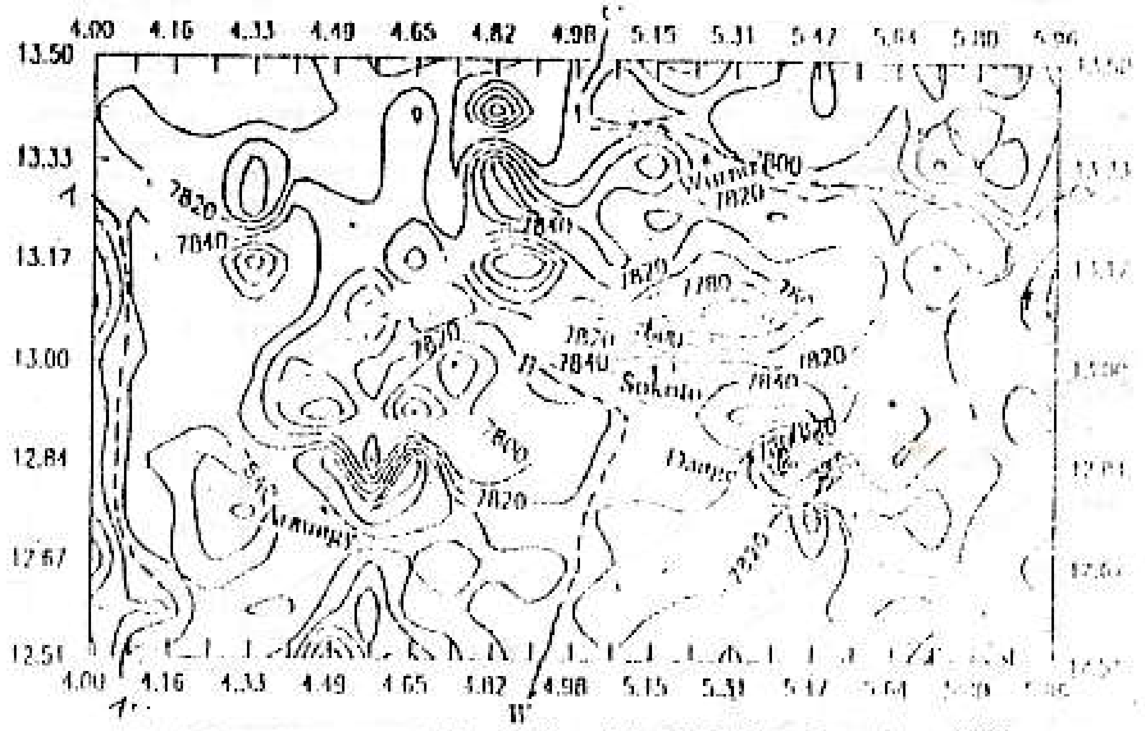

Fig. 5: Composite Aeromagnetic Map of the Upper Sokoto Basin (Contour interval = 20nT)

Qualitative Description of the Magnetic Anomalies in the Study Area

A critical look at Fig. 5 shows that a high frequency magnetic anomaly that is circularly shaped and is situated in the northwestern part of Dange. Southwestern Dange is characterized by low frequency anomalies: this may be attributed to deep-lying basement. Short and fairly long discontinuities exist within the study area and these are:

a. A-A is a N-S treading discontinuity within latitude 13.33° and longitude 4.00° to latitude 12.51° and longitude 4.08°. B-B is another N-S treading discontinuity in the western part of Dange within latitude 13.00° and longitude 4.82° to latitude 12.51° and longitude 4.98°

b. C-C' is NW-SE treading discontinuity within latitude 13.50° and longitude 4.98° to latitude 13.28° and longitude 5.96°.

these discontinuity indicate the short to moderately long fault zones that exist within the basement complex of the Upper Sokoto Basin.

Regional-Residual Separation

A magnitude is never a simple picture of a single isolated disturbance but superposition of disturbances of noticeably different orders of size i.e. the potential field observed over an area is a combination of a regional component and residual component. The regional component is that component of the total field arising from larger and generally deeper features while the residual components of the field are that component due to relatively local near surface masses. Thus magnetic interpretation frequently begins with separation of regional anomalies from the total magnetic anomalies to obtain the residual anomalies. The anomaly separation produce which is analogous to filtering of residual or "noise" from the smooth regional effect is achieved by either of the two methods of graphical or analytical. The analytical method involves a numerical procedure applied to an array of values on a regular grid.

Spectral Analysis of the Residual Field

Spectral analysis of the residual field data can be used to determine depth to buried magnetic rocks. These depths are usually computed from field observations made on the width and slopes of individual anomalies. Residual total magnetic field intensity values are used to obtain the two-dimensional Fourier series consisting of various frequencies which characterize the anomalies. It has been recognized recently that a statistically oriented approach is preferable because more than one anomaly can be used to determine depth to rocks. This approach has been found to yield god estimates of mean depth to the basement underlying a sedimentary basin (Treital et al. 1971, Hahn et al, 1976).

Historically, statistical spectral analysis of geophysical phenomena in the true sense of it hardly began before large capacity electronic computers came into more general use. And this was within the last fifty years. Spector and Grant (1970) developed a depth determination method. The regional map Fig. 6 of the study area trends NW-SE while the residual magnetic map (Fig.7) shows that the magnetic field over study area has no distinct trends.

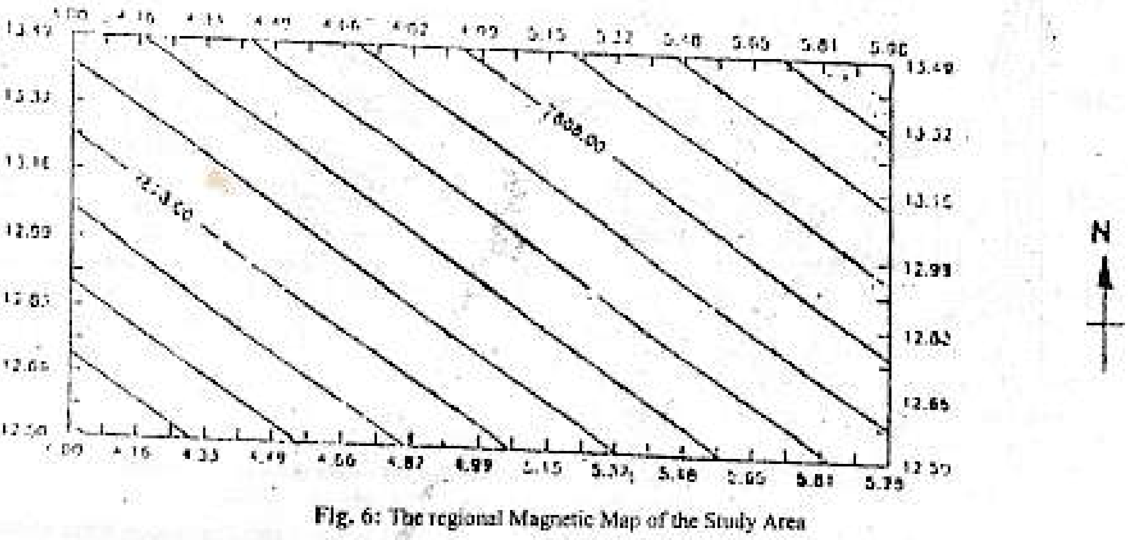

Fig. 6: The regional Magnetic Map of the Study Area

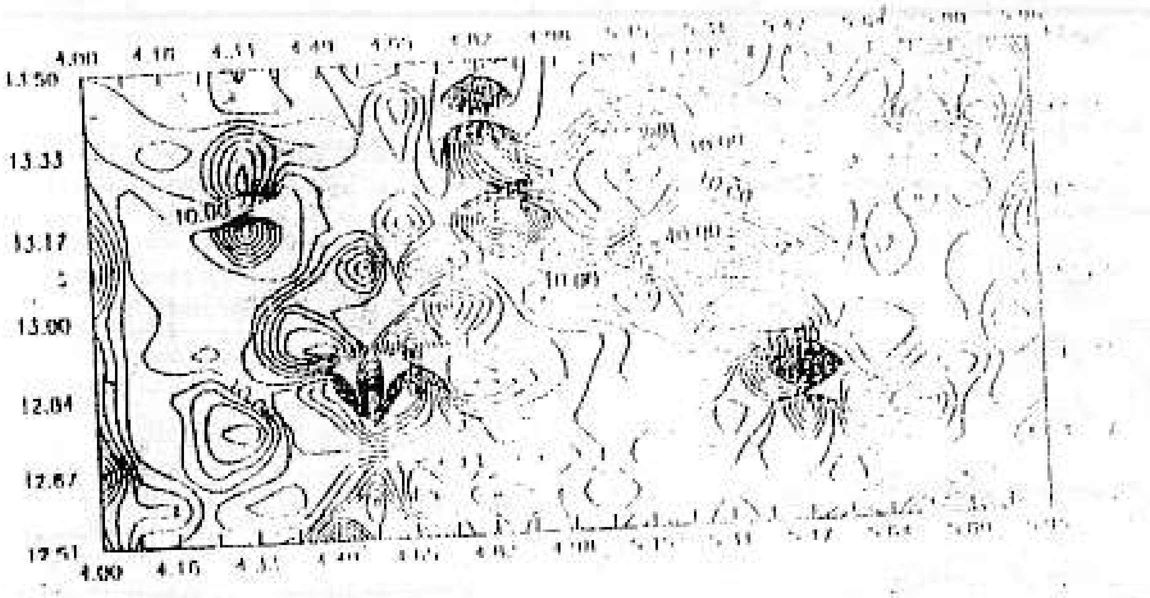

Fig. 7: The Residual Magnetic Map of the Study Area

Many of the anomalies in the residual magnetic map of Fig.7 have short wavelength, small widths and are more or less circular in the underlying basement surface. Series of closures are easily observed in the residual map with the steepest slope at the south eastern portion of the map latitude 13.00° - 12.67° and longitude 5.47° . The nature of these closures is indications of the depth to burial by the basin. Fairly long discontinuity exist between latitudes 12.51° to 13.33°. This discontinuity is an indication of possible faults zones within the basement complex of the basin.

Fundamentals of Spectral Analysis

The magnetic field is a function of two space variables X and Y due to vertical field and horizontal field. The dimension of the area along X and Y are normally finite and two consecutive points, of the digitized data are spaced apart by a finite interval. It is possible to present this data accurately by a two dimensional Fourier series which is bounded by lower and upper frequency limits because of the finite dimensions of the chosen area on one hand and the finite station spacing on the other. The least squares method was applied to the study area. Because the study area does not have complex geology and it has limited spatial extent, it seem adequate and reasonable to assume that the regional field is a first degree polynomial surface. All regional were therefore calculated s a two-dimensional first-degree polynomial surface.

The Fourier series consists of series of different frequencies that combine together to form the potential field data. The amplitude and phase relationships among these frequencies constitute what is called the complex line spectrum (Negi et al, 1983). These relationships govern the way the Fourier series is built up (Bhattacharyya, 1966) and it has been used extensively by various workers for the interpretation of gravity and magnetic data. A periodic function f(x) of the independent variable x, the dimension of which is length, may be expressed as a Fourier series as shown below:

$$f(x) = \frac{a_0}{2} + \sum_{n=1}^{\infty} \left(a_n \cos n\varpi x + b_n \sin n\varpi x\right) \quad 1$$

Where ϖ is the fundamental angular frequency given by $\varpi = 2\lambda / x$ and x is the total length of length over which f(x) has been measured. The coefficients a_n and b_n are given below:

$$a_n = \frac{2}{x} \int_{-x/2}^{x/2} f(x) \cos n\varpi x \, dx$$

and

$$b_n = \frac{2}{x} \int_{-1/2}^{1/2} f(x) \sin n\varpi x \, dx$$

Expressed in the exponential form Fig.1 may be written as

$$f(x) = \sum F(n) e^{in\varpi} \qquad 2$$

and

$$F(n) = \frac{1}{x} \int_{-1/2}^{1/2} f(x) e^{-in\varpi} dx \qquad 3$$

The amplitude spectrum of G(u,v) is

$$A(u,v) = /G(u,v)/ = [P^2+Q^2]^{1/2} \qquad 4$$

And its phase spectrum is

$$\Theta(u,v) = \arctan(Q/P) \qquad 5$$

The energy density spectrum or the energy spectrum is

$$E(u,v) = /G(u,v)/ = (P^2+Q^2) \qquad 6$$

For the treatment of sampled data the discrete form of g(u,v) has to be employed. Generally, the discrete Fourier transform pair for the two dimensional data sequence G(m,n) which is zero outside the interval $0 \le m \le M-1$, $0 \le n \le N-1$ is given by (Oppenheim and Schafer, 1975):

$$G(K,L) = \sum_{M=0}^{M-1} \sum_{N=0}^{N-1} g(m,n) \varpi_m^{-km} W_n^{l\cdot n} \qquad 7$$

$$g(m,n) = \frac{1}{MN} \sum_{M=0}^{M-1} \sum_{N=0}^{N-1} G(K,L) \quad \varpi_m^{-km} W_n^{l\cdot n}$$

8

$$\text{where } \varpi_m = \ell^{-\sqrt{\frac{2\pi}{m}}} \text{ and } W_n = \ell^{-\sqrt{\frac{2\pi}{n}}}$$

9

Energy Spectrum and Depth to Magnetic Source.

The Fourier transformation of a selection of magnetic map digitized in a square grid form a rectangular matrix with coefficients which can be reduced to a set of average amplitude dependent only on the frequency (Hahn et al, 1976). These average amplitudes fully represent the spectrum from which the depth to the magnetic source can be estimated. Consider the energy spectrum of the total magnetic field intensity anomaly over a single rectangular block. The expression for the energy spectrum transcribed in polar coordinates is given as follows (Spector and Grant, 1970):

If r=(u+v) and θ=arc tan(u/v)

Then the energy spectrum E(r, θ) is given by

$$E(r,\theta) = 4\pi^2 K^2 e^{-2hr}(1-e^{-tr}) S^2(r,\theta) R_T^2(\theta) R_K^2(\theta)$$

10

Where K is the magnetic moment per unit depth.

$$S(r,\theta) = \frac{\sin(ar\cos(\theta))}{ar\cos(\theta)} \frac{\sin(br\cos(\theta))}{br\cos(\theta)}$$

11

$$R_T^2(\theta) = [n^2 + (l\cos(\theta) + m\sin(\theta))^2]$$

12

$$R_K^2(\theta) = [N^2 + (L\cos(\theta) + M\sin(\theta))^2]$$

13

L,m,n are direction cosines of the magnetic moment vector. For the purpose of analyzing aeromagnetic maps, the ground is assumed to consist of a number of independent ensembles of rectangular, vertical sided parallelopiped, and each ensemble is characterized by a joint frequency distribution for the depth 'h'; width 'a' and length 'b' the overlapping sections consist of superposition of large number of individual anomalies overlapping due to several ensembles of blocks having various dimension and magnetizations.

The energy of the double ensemble will consist of two parts. The first, which relates the deeper source, is relatively strong at the low frequencies and decays away rapidily. The second, which arise from the shallower ensemble of source, the high frequence and of the spectrum. Spector and Grant (1970) obtained the expression for the ensemble average of the radial spectrum as

$$\langle E(r)\rangle = 4\pi^2 K^2 \langle \ell^{-2hr} \rangle \langle (1-\ell^{-tr})^2 \rangle \langle S^2(r) \rangle$$

14

$$\langle S^2(r)\rangle = \frac{1}{\pi} \int_0^{\pi} \langle S(r,\theta) \rangle d\theta$$

15

The ensemble average depth 'h' enters only into the factor:

$$\langle \ell^{-2hr} \rangle = \frac{\ell^{-2hr} \sinh(2r\Delta h)}{4r\Delta h}$$

16

Depth to magnetic rock estimations for magnetic data can be approximated to exp (-2hr)

(Spector and Grant). This shows that the radial spectrum may be conveniently approximated by a straight line segment, the slopes of the which relate to the depths of the possible layers (Spector and Grant 1970, Naidu, 1970 and Han et at 1976).

The residual total magnetic field intensity values are used to obtain the two dimensional Fourier Transform from which the spectrum is to be extracted from the residual values T (x,y) consisting of M row and N columns in the x-y plane, the two dimensional Fourier transform obtained in Eq.14 above and the evaluation is done using an algorithm that is a two dimensional extension of the fast Fourier transform (Oppenheim and Schafer, 1975. Cooley and Turkey, 1965). Next the frequency intervals are subdivided into sub-intervals, which lie within one unit of frequency range. The average spectrum of all the partial waves falling within the frequency range is calculated and the resulting values together constitute the radial spectrum of the anomalous field (Hahn et al, 1976, Negi et al, 1983, Kangkolo, 1996). The natural logarithm of the radial spectrum for each block were then plotted against frequencies. This plot showed a series of points that may well be represented by a straight lines (linear segments). Most of the points due to anomalies caused by the bodies occurring within a particular depth range or at different levels fall on one or more straight line segments whose slope can be used to determine the mean depth to the assemblage of anomalous bodies (spector and Grant, 1970 and the Hahn, et al. 1976). The first view points of low frequency components in the spectra graph, were generated from the deepest layers whose locations most likely in error were ignored, since it has been established that error in depth estimation increases with depth of source (Pal et al, 1978). The slope of segment is related to the depth as follow (Spector and Grant, 1970).

$$Z = -m/2$$

17

Where Z is the mean depth of the burial of ensemble and is the slope of best fit.

Eq.23 is the basic equation for the slope relation for power spectrum analysis and can be applied directly if the frequency unit is in radian per kilometer. If however, the frequency unit is in cycles per kilometer, the corresponding relation is expressed as

$$Z = -m/4\pi$$

18

The use of Discrete Fourier Transform (DFT) introduces the problem of Aliasing and the truncation effect (or Gibb's phenomenon) aliasing was reduced by the digitalizing interval used in this study. Truncation effect was reduced by applying a cosine taper to the observed data before Fourier transformation (Bath, 1974 and Kangkolo, 1996).

Application and Result

In order to spectrally determine depth to layer of magnetization the study was divided up into 60 overlapping sections. The locations of the sections are indicated in Tables 1 to 4. each section covers area of about 28km x 28km which represents a square grid of 14 x 14 residual field point. A computer programme, SPT 98, was then used to evaluate radial spectrum for each section.

Table 1: Location and Magnitude of first and Second Layer Average Depth for Map.

SECTION	LONGITUDE(Degree)	LATITUDE(Degree)	d 1 (km)	d 2(km)
01	4.00 - 4.25	13.25 – 13.50	0.42	1.64
02	4.25 - 4.50	13.25 – 13.50	0.67	1.18
03	4.50 - 4.75	13.25 – 13.50	0.41	1.36
04	4.75 - 5.00	13.25 – 13.50	0.34	1.23
05	5.00 - 5.25	13.25 – 13.50	0.33	1.50
06	5.25 – 5.50	13.25 – 13.50	0.65	1.04
07	5.50 – 5.75	13.25 – 13.50	0.62	1.27
08	5.75 – 6.00	13.25 – 13.50	0.19	1.22
09	4.00 - 4.25	13.00 – 13.25	0.34	0.82
10	4.25 - 4.50	13.00 - 13.25	0.51	1.31
11	4.50 - 4.75	13.00 – 13.25	0.55	1.17
12	4.75 – 5.00	13.00 – 13.25	0.58	1.98
13	5.00 - 5.25	13.00 – 13.25	0.15	1.40
14	5.25 - 5.50	13.00 – 13.25	0.25	0.76
15	5.50 - 5.75	13.00 – 13.25	0.31	0.34

Table 2 : Location and Magnitude of first and second layer average depth for map Sections 16 to 30

SECTION	LONGITUDE(Degree)	LATITUDE(Degree)	d 1 (km)	d 2(km)
16	5.75 – 6.00	13.25 – 13.50	0.20	1.99
17	4.00 – 4.25	12.75 – 13.00	0.21	1.16
18	4.25 – 4.75	12.75 – 13.00	0.42	1.14
19	4.75 – 4.75	12.75 – 13.00	0.28	1.72
20	5.00 – 5.25	12.75 – 13.00	0.18	1.10
21	5.25 – 5.50	12.75 – 13.00	0.21	1.98
22	5.50 – 5.75	12.75 – 13.00	0.41	0.59
23	5.75 – 5.75	12.75 – 13.00	0.20	1.99
24	4.00 – 4.25	12.75 – 13.00	0.46	0.52
25	4.25 – 4.25	12.75 – 13.00	0.46	1.52
26	4.50 – 4.75	12.75 – 13.00	0.26	1.15
27	4.75 – 5.00	12.50 – 12.75	0.43	1.14
28	5.00 – 5.27	12.50 – 12.75	0.24	0.73
29	5.25 – 5.50	12.50 – 12.75	0.21	1.57
30	5.25 – 5.50	12.50 – 12.75	0.19	0.89

Table 4: Location and Magnitude of First and second Layer average depth for Map section 46 to 60.

SECTION	LONGITUDE(Degree)	LATITUDE(Degree)	d 1 (km)	d 2(km)
46	5.25 – 5.50	12.875 – 13.125	0.23	0.90
47	5.50 – 5.57	12.875 – 13.125	0.42	1.20
48	5.75 – 6.00	12.875 – 13.125	0.27	1.33
49	4.00 – 4.25	1.625 – 12.875	0.36	1.14
50	4.25 – 4.50	1.625 – 12.875	0.30	1.30
51	4.50 – 4.75	1.625 – 12.875	0.51	1.15
52	4.75 – 5.00	1.625 – 12.875	0.17	1.00
53	5.00 – 5.25	1.625 – 12.875	0.20	1.47
54	5.25 – 5.50	1.625 – 12.875	0.36	1.69
55	5.50 – 5.75	1.625 – 12.875	0.25	1.20
56	5.75 – 6.00	1.625 – 12.875	051	1.50
57	4.125 – 4.375	12.500 – 12.750	0.62	1.87
58	4.375 – 4.265	12.500 – 12.750	0.45	1.58
59	4.625 – 4.875	12.500 – 12.750	0.35	1.17
60	4.875 – 5.125	12.500 – 12.750	0.27	1.09

Some of the sample graph of the logarithms of the spectral energies against frequencies obtained for the various sections are shown in Fig.8. Each of these graphs represents two linear segments. The first few points which represent contributions from much deeper

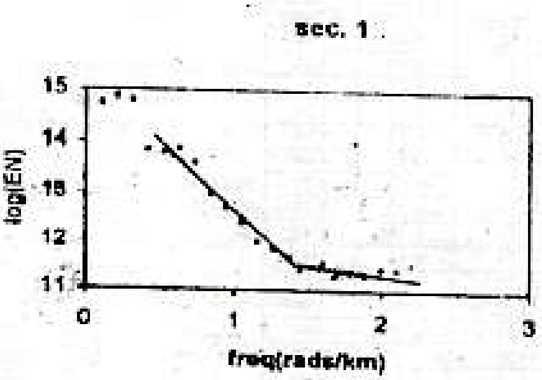

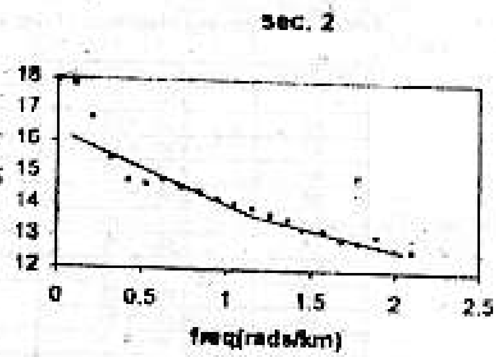

Fig. 8: Energy Spectra of various sections

Sources were ignored because of the reduced dimensions of these areas covered by these sections. As mentioned earlier, the gradient of the linear segment were evaluated and Eq. 23 was used to calculate the average depth to the causative bodies. From the earth surface downwards, this average depth are shown as d1 and d2 in Table 1 to 4. the first layer (d1) varies from 0.10km to 0.61km with an average of 0.367km. the second layer(d2) varies from 0.34km to 1.99km with an average of 1.368km. contour maps of the first layer (d1) and the second layer(d2) spectra values were obtained. Thus d2 values were used to obtain an approximate contour map of the basement surface in the basin. The contour maps of the first and second layers are shown in Figures 9 and 10 respectively.

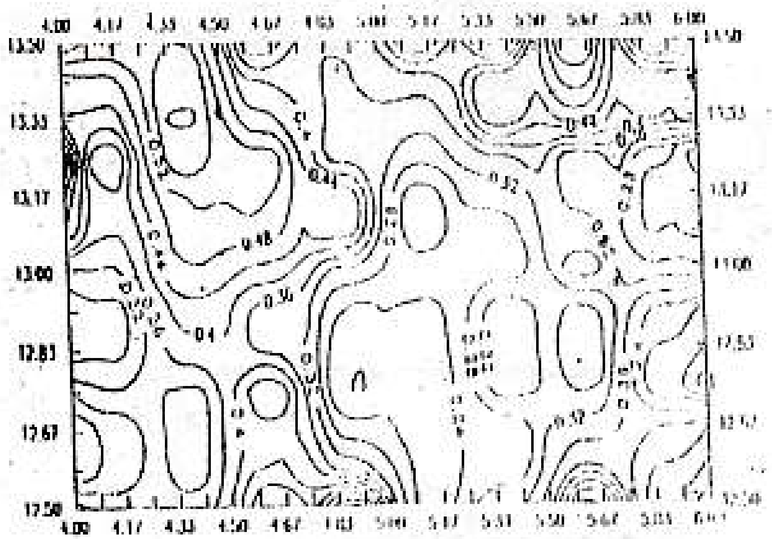

Fig. 9: First Magnetic Layer (d1) Depth Countour Map (Countour interval = 0.04km)

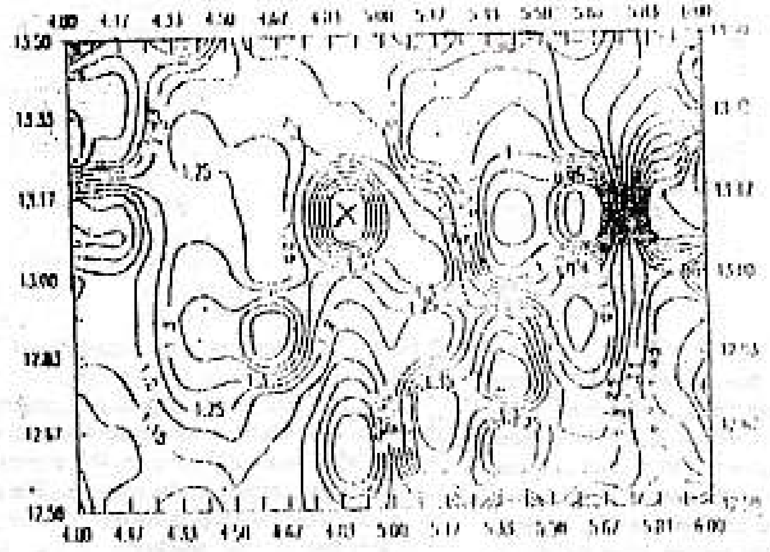

Fig. 10: Second magnetic layer (d_2) Depth Contour Map (Countour interval = 0.05km)

From the depth values (d1 and d2) the surface plots of first and second layer were generated. The plots are shown in Figures 11 and 12 respectively with the ground surface regarded at a depth 0.00km.

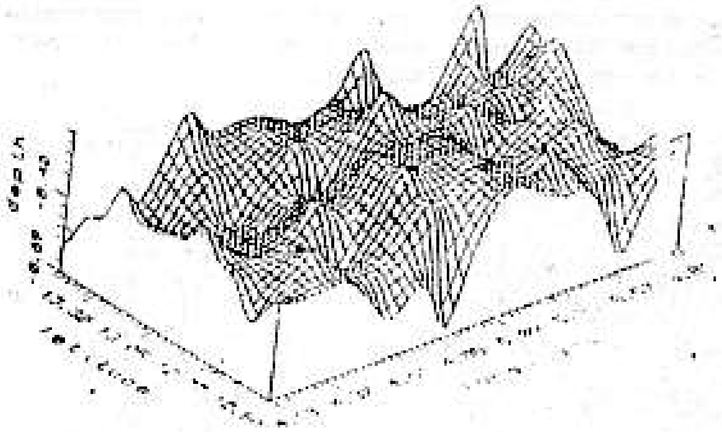

Fig.11: Surface plots of First Magnetic layer

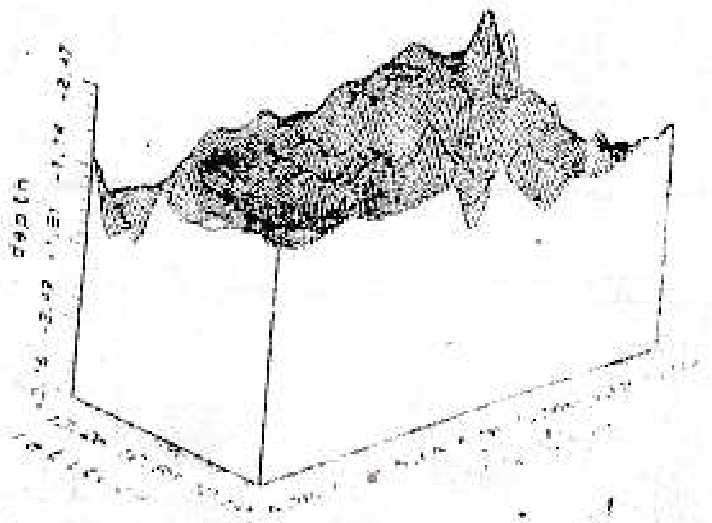

Fig. 12: Surface Plots of Second Magnetic Layer

Discussion of Result

It is important to note that spectra depth are in general average depth and individual depth estimates may have values which differ from these depths. The analyses in tables 1 to 4 indicates that first layer depth i.e. depth to the top of the intrusion causing the anomalies are at depth laying between 0.10km and 0.61km and the second layer depth, i.e. depth to the bottom intrusion range from 0.34km and 0.99km.

The first layer depths d1represent average depth to the shallow magnetic horizon while the second layer depth d2 represent the average depth to the basement complex in the sections. The average in the study were calculated to be 1.386km. this also represent the average thickness of the sedimentary formation overlaying the basement complex within the upper Sokoto basin. Umego(1990) stated from preliminary interpretation of gravity measurement within the basin that the maximum possible thickness of the sedimentary section in Sokoto basin is no where considered to exceed 2km.

Fig.10 is the contour map of the second magnetic layer and it indicates in generally shallow and low relief structure with gentle undulation. A careful look at fif.10 shows that the anomalies over the study area are of low frequency and gradient which s suggestive of either a deeper sources horizon or uniform magnetic properties of the underlying basement rock. A further look at the contour map of the second layer depth shows the presence several closures. These closures represent 3-D features. The area with the highest thickness of sedimentary fill is marked 'X' and it is located nearly at the center point of fig.10. Its sedimentary thickness is about 1.99kmwith general increase in depth from west to east of the study area.

Conclusion

The procedure used in this work is based of the method developed by Spector and Grant (1970). The residual total magnetic field intensity values are used to obtain the two dimensional Fourier transform from which radial spectrum were extracted. From the slope of the graph of the logarithms of spectral energy against frequency, 60 sections were obtained and the average depth of Sokoto basin was determine by the slope values.. the result of spectral analysis of the residual data field reveals two clear layers of magnetic source. The first layer depth varies between 0.1km-0.61km and are of shallow magnetic horizon represented by the low frequency component of the spectrum are considered to reflect the depth to the magnetic basement. From the second layer depth it can be conducted that the thickness of sedimentary formation overlying the basement complex in the upper Sokoto basin vary from about 0.34km to about 1.99km with an average of 1.386km.

The result of this research correlates well with the result of Umego (1990) who used Werner Deconvolution method and got sediment thickness range of 1.2km to 1.8km. it also correlates well with Ojo and Ajakaiye (1976) which stated that the basement depth is no where greater than 2km within the Nigeria cretaceous sediments. The Sokoto basin is composed of cretaceous sediments as well. The surface plot of Fig.12 is generalized depth to magnetic basement. It reveals a generally shallow basement surface deepest with a maximum depth of 1.99km. it extends from latitude 13.00 to latitude 13.25 and longitude 4.50 to 6.00 in the northeast central of the study area and gradually diffused in a decreasing order towards the eastern and western boundaries. This diffuse nature of the surface plot is an indication of tectonic events with N-S trend and ridges in the southwestern part of the study area. On the surface plot of Fig.12, depression varies in depth between 0.73km and 0.98km in the study area. This agrees with the gravity result of Umego (1990) which estimated depression to have a depth 10km. the economics significant of this result is in the consideration of the hydrocarbon potential. It can be noted that the sedimentary thickness obtained in this analysis are rather small to allow for accumulation of hydrocarbon. A maximum thickness of 1.99km obtained in this study is less than 2.3km minimum depth recommended by Wright et al (1985) with threshold temperature of 115^{0}C for the accumulation of oil from organic deposit. Owing to shallow depth of the probable source bed in the basin there is no prospect in the basin.

Recommendation

Based on the result obtained from the spectra analysis of the magnetic residual anomalies for depth determination to the basement the following recommendation are made:

A detailed spectral depth determination with reasonable number of windows should be carried out in the lower section of Sokoto basin. This will give a general picture of sedimentary thickness in the basin. The use of the other geophysical technique such as seismic, resistivity, and well-logging in drilled boreholes should strongly encourage in the basin.

A detailed study of the Iullenmmeden basin by spectral depth analysis and modeling technique of magnetic data should be carried out with the aim of determine the origin, average depth, underlying structure and tectonic events of the basin of which the Sokoto basin forms as part.

References

Bath, M (1974): "Spectral Analysis in geophysics". Elsevier Publishing Co. Amsterdam, p563.

Bhattachaya, B.K. (1966): continuous spectrum of the Magnetic Field Anomaly Due to a Rectangular Prismatic Body", Geophysics 31, pp97-121.

Cooley, J. W. and J.W. Turkey, (1965): " An Algorithm for the Machine Calculation of Complex Fourier Series". Mathematics of Computation 19 pp297-301.

Hahn, A. E. G. Kind and D. C. Mishra.